coatings

MDPI

Article

The Influence of Two Spinning Processes of T800 Grade Carbon Fibers on the Mechanical Properties of Thermoplastic Composite Material

Xu Cui [1,2], Xuefeng Sun [2], Weiguo Su [3,*], Shuo Wang [2,*] and Han Guo [1]

[1] Liaoning General Aviation Academy, Shenyang 110136, China; cuixu@sau.edu.cn (X.C.)
[2] College of Aerospace Engineering, Shenyang Aerospace University, Shenyang 110136, China; sxf1209@outlook.com
[3] National Key Laboratory of Electromagnetic Energy, Naval University of Engineering, Wuhan 430033, China
* Correspondence: suweiguo1985@126.com (W.S.); shuowang@sau.edu.cn (S.W.)

Abstract: Two types of T800 grade carbon fibers, produced using distinct spinning processes, were utilized to fabricate thermoplastic prepregs via the hot melt method. These prepregs were subsequently employed to produce thermoplastic composites. A universal testing machine was used to assess the tensile, bending, and interlaminar shear properties of the composites, evaluating the impact of the two different spinning processes on their mechanical characteristics. The experimental results indicate that the dry spray wet spinning carbon fiber (T800-DJWS) exhibits a smoother surface, more regular cross-section, and more uniform distribution compared to the wet spinning carbon fiber (T800-WS), enhancing the prepreg preparation via the hot melt method. The T800-DJWS/PAEK composite demonstrates a tensile strength that is 706 MPa higher than the T800-WS/PAEK composite, while the latter exhibits a bending modulus 31 GPa higher than the former.

Keywords: T800 grade carbon fiber; prepreg; spinning processes; composite; mechanical properties

Academic Editors: Pinto Luiz Antonio de Almeida and Bruna Silva de Farias

Received: 27 December 2024
Revised: 10 January 2025
Accepted: 14 January 2025
Published: 15 January 2025

Citation: Cui, X.; Sun, X.; Su, W.; Wang, S.; Guo, H. The Influence of Two Spinning Processes of T800 Grade Carbon Fibers on the Mechanical Properties of Thermoplastic Composite Material. *Coatings* **2025**, *15*, 90. https://doi.org/10.3390/coatings15010090

1. Introduction

Carbon fibers, containing over 95% carbon, are inorganic polymer fibers recognized for their low density, high strength, temperature resistance, and fatigue durability [1–4]. Carbon fiber-reinforced thermoplastic composites exhibit properties including a high specific strength and modulus, thermal stability, corrosion and fatigue resistance, and weldability. These composites are extensively utilized in fields such as aerospace, military equipment, and vehicle manufacturing [5–8].

The T800 carbon fiber exhibits superior mechanical and tensile properties compared to the T300 and T700 variants. Yidong Zhang et al. found that the coefficient of variation of tensile strength was 5.49% by studying the fatigue properties of T800 carbon fiber/epoxy composites, and the coefficient of variation of tensile strength was found to be 5.49% by refining the fatigue life model of T800 carbon fiber/epoxy composites. The refined fatigue life model of T800 carbon fiber/epoxy plywood accurately predicted its fatigue life and the process of fatigue damage failure [9]. The T800 carbon fiber's high strength-to-weight ratio makes it ideal for aircraft manufacturing, especially in load-bearing components like wings, fuselages, and tails.

Prior to forming thermoplastic composites, fibers and resins are prepared as prepregs. Prepregs are primarily prepared via two methods: the solution and the hot melt techniques.

The hot melt method, known for precise resin content control, lower volatility, and minimal environmental impact, is favored for future prepreg production [10–14]. However, this method's application is challenging, limited, and highly dependent on the properties of raw materials. Composite performance can vary based on the spinning processes used to prepare the carbon fibers. Currently, carbon fibers are mainly prepared via two methods: wet spinning and dry-jet wet spinning [15–19]. In wet spinning, the spinning solution is filtered, degassed, and then precisely delivered to a spinning head submerged in a coagulation bath, where it solidifies upon extrusion [20–22]. However, increasing the drawing speed in wet spinning often leads to breakage at the spinneret, complicating speed enhancements and resulting in significant grooves on the surface of the spun silk. Dry-jet wet spinning, a novel technique, merges the features of both dry and wet spinning methods. Exiting the spinneret, the spinning solution passes through a dry air or nitrogen layer before solidifying in the coagulating liquid [23–26]. The dry-jet wet spinning process, which incorporates an extended air layer, promotes physical changes in the spinning solution that lead to a denser surface layer, preventing large holes and achieving more uniform fiber bundles. This method also supports extensive drawing, enhancing the strength of the produced silk.

This paper explores the optimization of the production process and the enhancement of material properties through a comparative analysis of two distinct spinning processes for carbon fibers. Concurrently, integrating thermoplastic composites with carbon fibers shows promise for enhancing material properties in the aviation and automotive sectors.

2. Experimental Section

2.1. Raw Materials

T800-WS carbon fiber (wet spinning), Shanxi Steel Research Institute of Carbon Materials Co., Ltd. (Datong, China); T800-DJWS carbon fiber (dry-jet wet spinning), Toray Industries, Inc. (Tokyo, Japan), see Table 1 for details. PAEK resin, Jiangsu Hengbo Composite Material Co., Ltd. (Quanzhou, China), see Table 2 for details.

Table 1. Multifilament properties of T800 grade carbon fibers used in two spinning processes.

Fibre Grade	Tensile Strength (MPa)	Tensile Modulus (MPa)	Elongation (%)	Surface Sizing Agent Content (%)
T800-WS	5463	292	2.10	1.18
T800-DJWS	5972	294	2.32	1.08

Table 2. Performance of PAEK.

Resin Grade	Viscosity (360 °C) (Pa·s)	Melting Point (g/m^2)	Tg (%)
PAEK	423	314	147

2.2. Specimen Preparation

(1) T800-WS and T800-DJWS carbon fibers were used as reinforcing materials, and PAEK resin as the matrix resin. T800-WS/PAEK and T800-DJWS/PAEK prepregs are produced using a hot melt process that involves heating PAEK resin to 343 °C in an extruder, followed by impregnating T800 fibers in a bath of molten resin to achieve uniform coverage. The impregnated fibers are then cooled to cure the resin. After cooling, calendaring rollers refine the resin's surface to improve fiber–resin adhesion. The glass transition temperatures of both T800-WS and T800-DJWS carbon fibers are indistinguishable, and the finished prepregs are displayed in Figure 1, with the relevant properties shown in Table 3. The prepregs were finalized at a size of 120 × 40 × 0.2 mm.

Figure 1. T800-WS/PAEK prepreg and T800-DJWS/PAEK prepreg.

Table 3. Properties of prepregs prepared by two spinning processes using T800 grade carbon fiber.

Prepreg Grade	Resin Content (%)	Fiber Surface Density (g/m^2)	Volatility (%)	Thickness (mm)
T800-WS/PAEK	36.5	144.8	0.13	0.2
T800-DJWS/PAEK	34.2	144.1	0.11	0.2

(2) The T800-WS and T800-DJWS prepregs were found to contain epoxy sizing agents. The surface sizing agents were removed through the process of complete immersion in acetone for two hours, followed by washing with deionized water. The curing temperature profile shown in Figure 2 was established in accordance with the PAEK matrix Tm = 317 °C, with the objective of ensuring the material's fluidity within the mold. The thickness of each specimen was 2 mm.

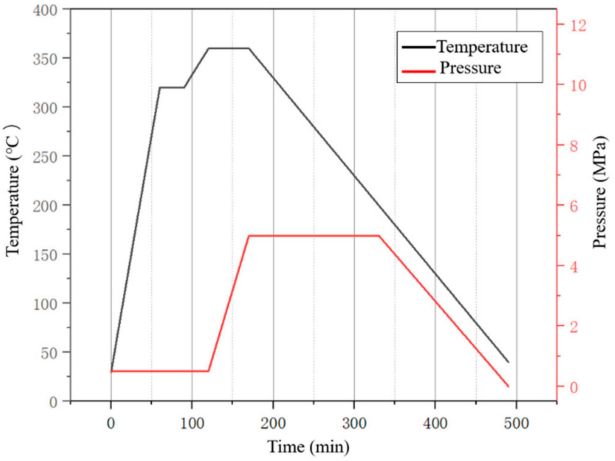

Figure 2. Composite curing preparation curve.

2.3. Performance and Testing Methods

2.3.1. Tensile Property Testing

The tensile properties of the T800-WS/PAEK and T800-DJWS/PAEK composites were tested using a YHS-WE-300B-1 universal testing machine (Chengyu Test Equipment Co., Jinan, China) in accordance with the QJ971A-2011 standard [27]. The dimensions of the specimens utilized in the experimental phase of this study were precisely measured at 200 × 15 × 2 mm. The tensile test was methodically performed on each specimen five times to ensure the reliability of the experimental results.

2.3.2. Bending Property Testing

The flexural properties of the T800-WS/PAEK and T800-DJWS/PAEK composites were examined through a series of five tests, employing the YHS-WE-300B-1 universal testing

machine in accordance with the GB/T3356-1999 standard [28], as illustrated in Figure 3a. The test specimens, each measuring 70 × 10 × 2 mm, were subjected to a bending test.

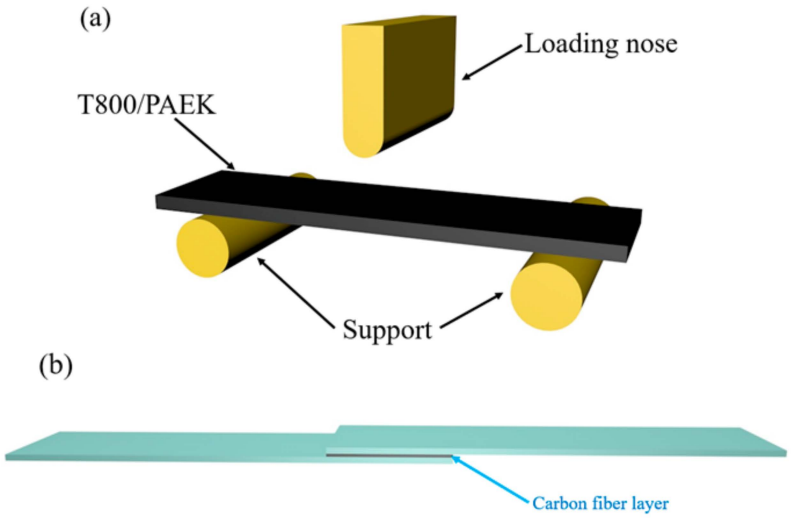

Figure 3. (**a**) Flexural test model, (**b**) shear strength test model.

2.3.3. Interlaminar Shear Strength Testing

According to the JC/T773-2010 standard [29], the YHS-WE-300B-1 universal testing machine was used to test the interlaminar shear strength of the T800-WS/PAEK and T800-DJWS/PAEK composites. The experimental setup for the interlayer shear test is shown in Figure 3b. Each experimental specimen's size was 8 × 10 × 2 mm, and the experiment was repeated five times.

2.3.4. Microscopic Analysis

It is crucial to keep the surface of each experimental sample clean and dry. We applied platinum to each sample's surface by spraying. Subsequently, we used a scanning electron microscope (SEM, Hitachi SU8020, Tokyo, Japan) to examine the fracture surface morphology of five specimens from each mechanical experiment at a scanning voltage of 10 kV.

3. Results and Discussion

3.1. The Impact of Two Spinning Processes of T800 Grade Carbon Fiber on Prepreg Preparation

According to the properties of carbon fiber filaments, both dry-jet wet spinning and wet spinning yield similar tensile moduli and elongation. However, T800-DJWS exhibits a 9.3% higher tensile strength than T800-WS. To analyze this further, the sizing agent was removed from the fibers' surfaces using a solvent, and their microscopic surfaces were examined using a scanning electron microscope. Figure 4 illustrates that the T800-DJWS filament bundle has a smoother surface compared to the rough and uneven surface of the T800-WS filament bundle, highlighting a significant difference between the two processes. In the spinning process, dry-jet wet spinning introduces an air layer that forms a dense protective layer on the fiber surface upon extrusion from the nozzle, thus minimizing surface wear. Consequently, fibers produced by dry-jet wet spinning have smoother surfaces and higher tensile strength than those produced through wet spinning. Figure 5 displays gold micrographs of the fibers' cross-sections, where T800-DJWS features a uniform filament distribution and a circular cross-section, in contrast to T800-WS's dispersed and uneven distribution and its oval or pea-shaped cross-section. During wet spinning, lacking an air layer's protection, fibers often cling to the filament bundle's outer edge due to electrostatic forces. Subsequently, the outer filament bundle becomes dense, while the inner bundle remains loose. However, dry-jet wet spinning mitigates electrostatic adhesion under the air

layer's protection, leading to more uniform fiber distribution post-spreading. Moreover, the significant friction in wet process fibers results in elliptical or pea-shaped cross-sections, rather than irregular and circular ones.

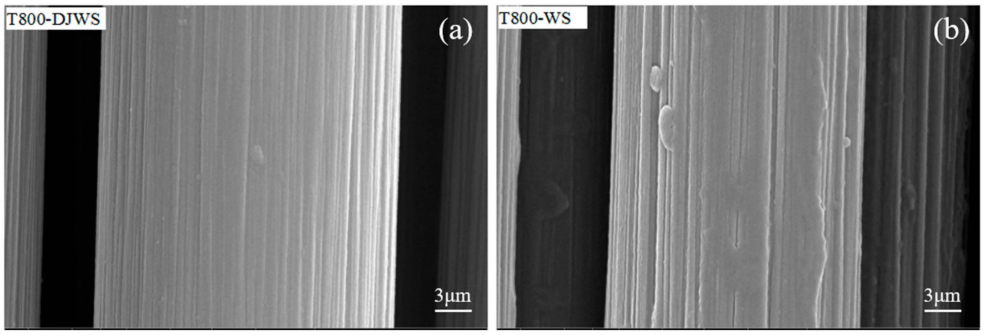

Figure 4. SEM images of carbon fibers with surface sizing agent removed: (**a**) T800-DJWS, (**b**) T800-WS.

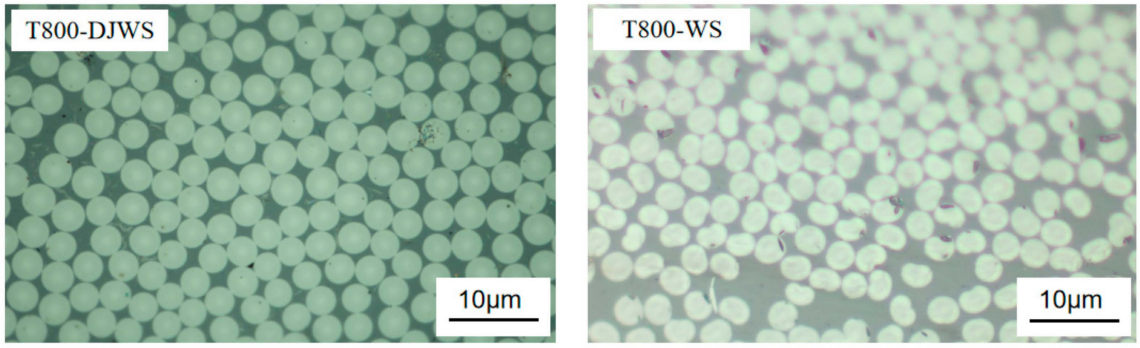

Figure 5. Metallographic images of T800 grade fiber cross-sections prepared by two different processes.

Two types of carbon fiber fabrics were converted into 100 mm wide prepregs using the hot melt method, as depicted in Figure 1. Visually, both prepregs appeared similar in quality, without evident issues like excess or insufficient resin, gaps, fuzz balls, or folds. The consistent prepreg fabrication process does not compromise the quality of the prepregs or introduce local defects. Figure 6 presents a cross-sectional view of the prepreg. The T800-WS/PAEK prepreg, based on T800-WS, displays notable local defects such as resin deficiency and excess. Conversely, the T800-DJWS/PAEK prepreg, based on T800-DJWS, shows a uniform resin and fiber distribution with no significant gaps. In the T800-WS/PAEK prepreg, the fibers are loosely arranged, mirroring the distribution in a single T800-WS fiber bundle. The external surface of this bundle is resin-rich, whereas the internal area lacks resin, or, conversely, the internal area is resin-rich and the external surface has less resin. In the prepreg fabrication process, hot melt resin is applied to the fiber surface using the impregnator's squeeze head, then rolled with a high-temperature heating roller. When fibers in the bundle are unevenly dispersed, the viscous resin flows and accumulates in areas of looser fiber distribution within the cross-section. The remaining resin is applied to the fiber bundle's surface; however, due to the minimal resin content and low squeezing force, the internal fibers are not fully impregnated, resulting in resin-rich outer fibers and poorly impregnated internal areas. The T800-DJWS fibers are uniformly distributed, resulting in a consistent resin and fiber arrangement in the prepreg, with virtually no issues of insufficient resin or bonding.

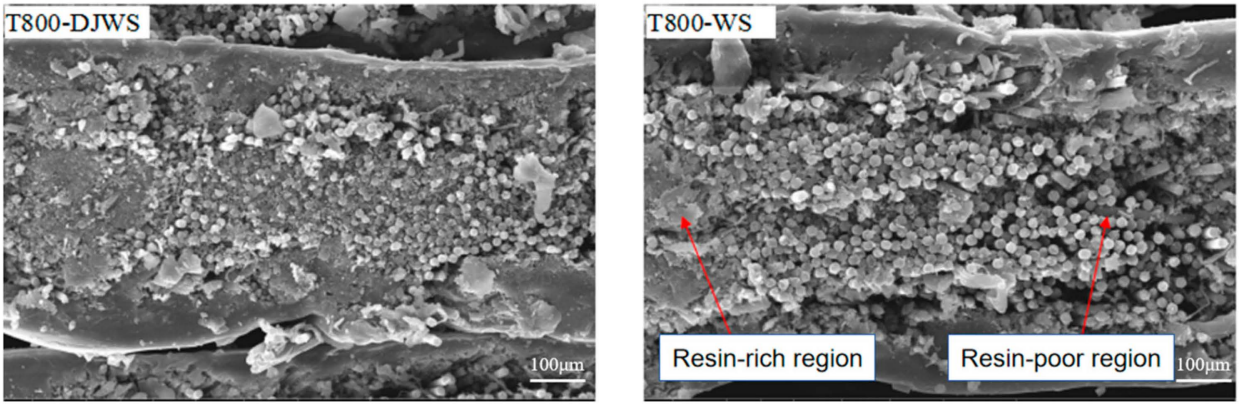

Figure 6. Electron microscopic images of T800-DJWS/PAEK prepreg and T800-WS/PAEK prepreg.

3.2. The Effect of Two Spinning Processes on the Mechanical Properties of T800 Grade Carbon Fiber-Reinforced Thermoplastic Composites

3.2.1. Tensile Properties

As demonstrated in Figure 7, the tensile strength of T800-DJWS/PAEK composites is considerably higher than that of T800-WS/PAEK composites, reaching 2816 MPa. The tensile strength of T800-DJWS/PAEK composites exceeds that of T800-WS/PAEK composites, which is 706 MPa. Figure 8 illustrates that the failure patterns of the T800-DJWS/PAEK and T800-WS/PAEK tensile samples are similar, primarily characterized by fiber tensile failure. Upon applying a tensile load, the fiber and resin matrices in the composites undergo plastic deformation. The extension rates of both fibers are similar and lower than that of PAEK, resulting in nearly identical tensile modulus values for the composites. The failure analysis of the tensile samples indicates that the fibers break before the resin. Consequently, the tensile test ceases before the resin matrix sustains extensive damage. Consequently, the tensile strength primarily depends on the comparative tensile strength of the fibers. Table 1 compares the performance of the fiber filaments, indicating that the T800-DJWS fiber has higher tensile strength than the T800-WS fiber. Consequently, the T800-DJWS/PAEK composite exhibits superior tensile strength compared to the T800-WS/PAEK composite.

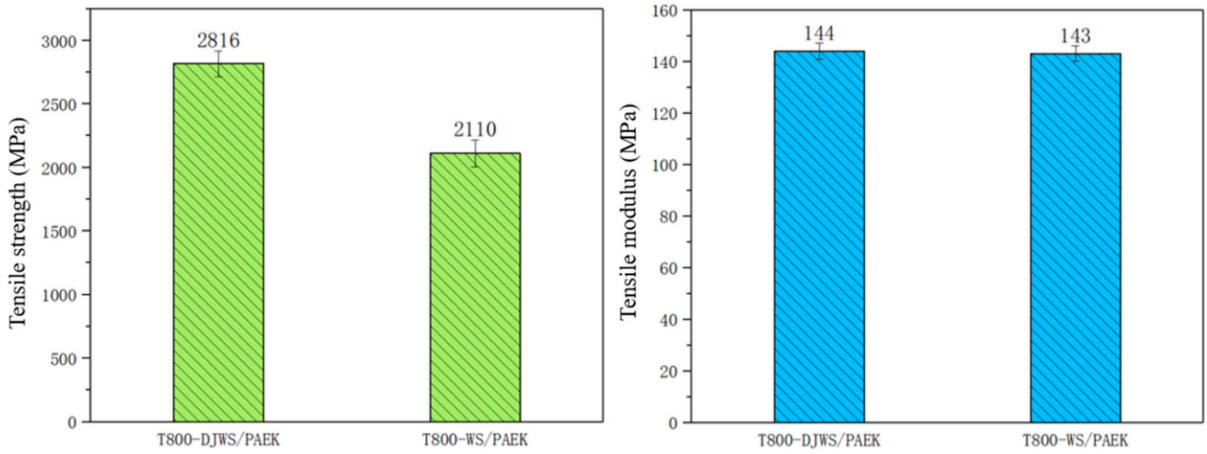

Figure 7. Tensile properties of T800-DJWS/PAEK composites and T800-WS/PAEK composites.

Figure 8. T800-DJWS/PAEK and T800-WS/PAEK composite samples that experienced tensile test failure.

3.2.2. Bending Performance

According to the bending modulus's definition, a smaller bending modulus results in less deformation and deflection of the composite material when bending strength remains constant. Figure 9 shows that the bending strength of the T800-DJWS/PAEK composite slightly exceeds that of the T800-WS/PAEK composite, with both values reaching approximately 1700 MPa. Figure 10 illustrates that the microscopic fracture patterns of the T800-DJWS/PAEK and T800-WS/PAEK specimens used in the bending tests are similar. The interfacial failure modes of both specimens are similar, suggesting that fiber stiffness predominantly determines their bending strength. The bending modulus of the T800-DJWS/PAEK composite is 31 GPa lower than that of the T800-WS/PAEK composite. Under identical loading conditions, the T800-DJWS/PAEK composite exhibits less deformation and greater stiffness compared to the T800-WS/PAEK composite. When the resin matrix composition is constant, the observed discrepancy in flexural strength is directly proportional to the inherent stiffness of the fibers. The higher regularity of the T800-DJWS fiber's cross-section compared to that of the T800-WS fiber results in increased stiffness, accounting for the differences in their bending moduli.

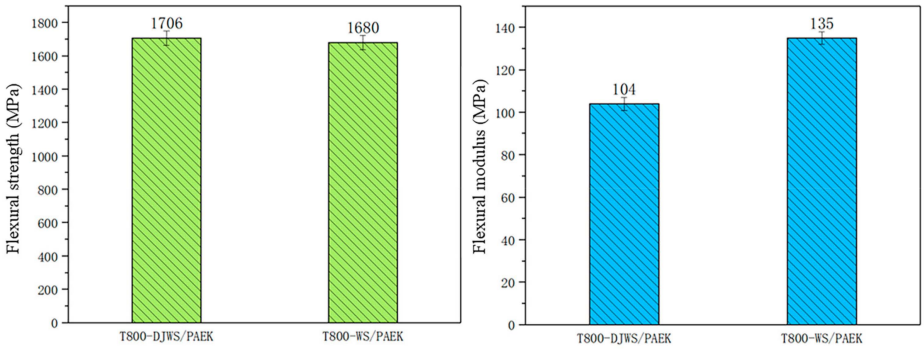

Figure 9. Flexural text results for T800-DJWS/PAEK and T800-WS/PAEK.

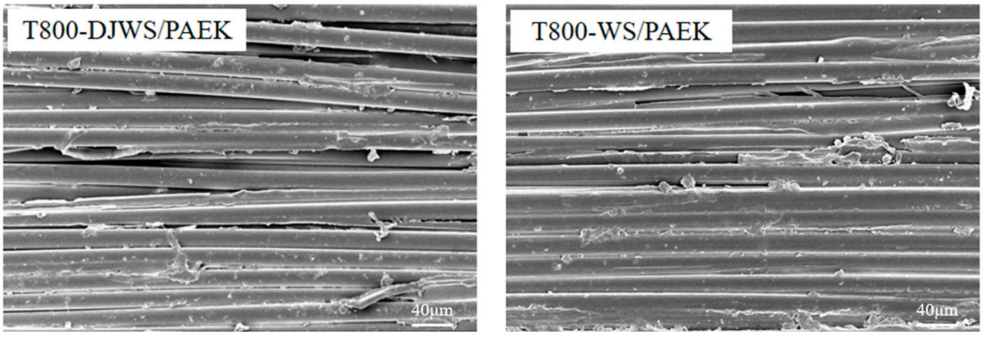

Figure 10. Electron microscope images of morphology of cross-sections of specimens after bending property test failure.

3.2.3. Interlayer Shear Performance

Interlaminar shear tests are primarily used to evaluate the bond strength between fibers and resin in composite materials. The rougher surface of wet carbon fibers increases the contact area and enhances mechanical interlocking between the fibers and resin in the microstructure. Consequently, this improves interfacial bonding between the resin and fibers during the mechanical hot-pressing process. However, the presence of an epoxy sizing agent causes the PAEK matrix to bind to this agent on the fiber's surface during curing instead of directly to the carbon fiber. The epoxy sizing agent is crucial for preventing damage, enhancing processability, improving interfacial adhesion, and ensuring a uniform, robust bond between the PAEK matrix and the fibers. A prerequisite for this effect is that the sizing agent on the carbon fibers must be compatible with the matrix resin. For epoxy resin matrices, epoxy sizing agents are appropriate, whereas specifically developed thermoplastic sizing agents are required for thermoplastic resin matrices. Using traditional epoxy sizing agents typically results in a weaker bond between carbon fibers and resin. Both of the domestic T800-level carbon fibers prepared via the two processes utilize epoxy resin as a sizing agent, resulting in their similarly weak interlaminar shear strengths, as depicted in Figure 11. Figure 12 displays an electron microscope image of the failure interface for a single fiber from each the composites prepared by both carbon fiber processes. The sizing agent's presence results in no significant roughness differences on the fiber surfaces. Both samples feature fibers (the symbol in question is a green oval) well-adhered with resin (the object in question is a red rectangular box with a dashed outline), without evident delamination, indicating uniform and ideal bonding conditions between the resin and the fibers and, thus, consistent interlaminar shear strength.

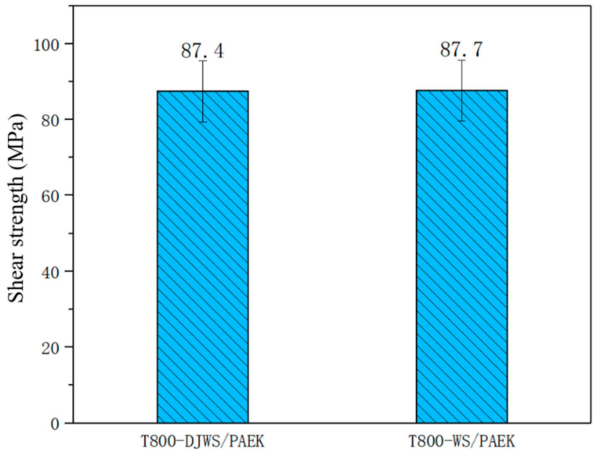

Figure 11. Shear strength test results for T800-DJWS/PAEK and T800-WS/PAEK.

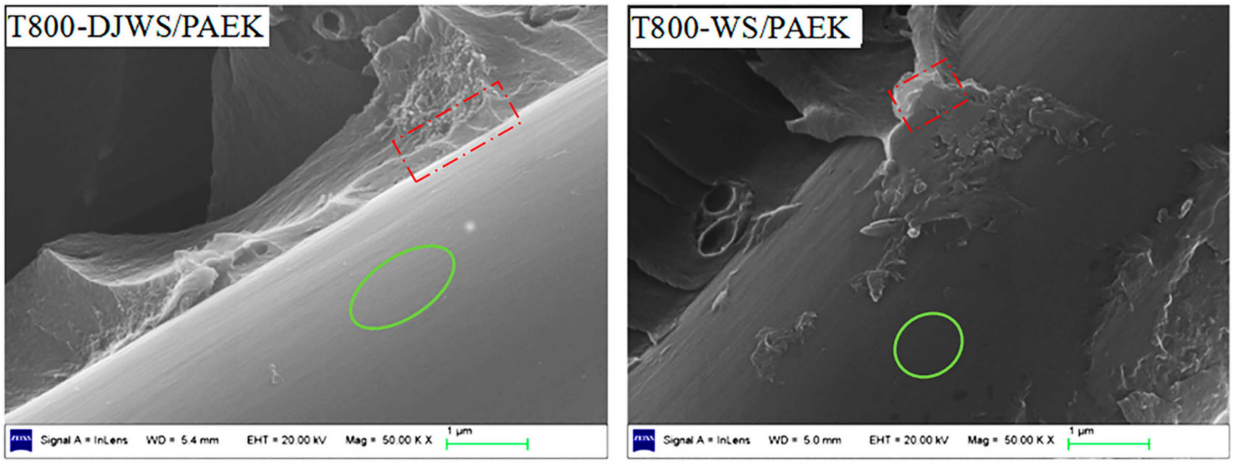

Figure 12. Interlayer shear sample cross-section failure SEM images (Fiber in green oval box, resin in red dashed rectangular box).

4. Conclusions

The preparation process of carbon fiber significantly impacts its mechanical properties and appearance, which, in turn, affects the performance and mechanical properties of the resulting composite material.

(1) T800-DJWS carbon fiber, produced via dry-jet wet spinning, features a smooth, grooveless surface with a regular, circular cross-section. Conversely, T800-WS carbon fiber, made by wet spinning, exhibits a rough surface with multiple grooves and an irregular, often elliptical or pear-shaped cross-section. The tensile strength of T800-DJWS is 706 MPa higher than T800-WS, with other properties being equivalent.

(2) The T800-DJWS/PAEK prepreg exhibits no surface defects, uniform fiber distribution, and effective resin impregnation, with all physical properties meeting specified standards. The T800-WS/PAEK prepreg, while also free of surface defects, shows internal variations with areas of insufficient and excessive resin. However, its physical properties remain within acceptable limits and do not impede normal usage.

(3) The tensile strength of the T800-DJWS/PAEK composite exceeds that of T800-WS/PAEK by 706 MPa, whereas the flexural modulus of T800-WS/PAEK is 31 GPa greater than that of T800-DJWS/PAEK. The bending strength of both is consistent with the interlaminar shear strength.

In summary, the main differences in the mechanical properties of thermoplastic composites prepared using various spinning processes are evident in their tensile strength and flexural moduli, with no notable variations in tensile moduli, flexural strength, or interlaminar shear strength. This study offers a detailed analysis of the impact of carbon fiber preparation processes on composite material properties. The results provide essential insights for engineers regarding material selection, manufacturing optimization, and structural design, facilitating enhanced composite performance and reliability that can meet stringent engineering standards.

Author Contributions: Conceptualization, X.S.; Methodology, X.C.; Validation, X.S. and W.S.; Investigation, H.G.; Resources, W.S. and S.W.; Writing—original draft, X.C.; Writing—review & editing, X.S.; Visualization, W.S.; Supervision, X.S.; Funding acquisition, S.W. All authors have read and agreed to the published version of the manuscript.

Funding: This work was financially supported by the Surface Project of the Liaoning Provincial Department of Education (no. JYTMS20230226).

Informed Consent Statement: Informed consent was obtained from all subjects involved in the study.

Data Availability Statement: Data are contained within the article.

Conflicts of Interest: The authors declare no conflict of interest.

References

1. Alshammari, B.A.; Alsuhybani, M.S.; Almushaikeh, A.M.; Alotaibi, B.M.; Alenad, A.M.; Alqahtani, N.B.; Alharbi, A.G. Comprehensive Review of the Properties and Modifications of Carbon Fiber-Reinforced Thermoplastic Composites. *Polymers* **2021**, *13*, 2474. [CrossRef] [PubMed]
2. Rafique, I.; Kausar, A.; Muhammad, B. Epoxy Resin Composite Reinforced with Carbon Fiber and Inorganic Filler: Overview on Preparation and Properties. *Polym-Plast. Technol. Eng.* **2016**, *55*, 1653–1672. [CrossRef]
3. Shoaib, M.; Jamshaid, H.; Alshareef, M.; Alharthi, F.A.; Ali, M.; Waqas, M. Exploring the Potential of Alternate Inorganic Fibers for Automotive Composites. *Polymers* **2022**, *14*, 4946. [CrossRef] [PubMed]
4. Jian, Z.; Wang, Y.; Zhang, X.; Yang, X.; Wang, Z.; Lu, X.; Xia, H. Fully recyclable high-performance polyacylsemicarbazide/carbon fiber composites. *J. Mater. Chem. A* **2023**, *11*, 21231–21243. [CrossRef]
5. Zhai, C.; Chen, Y.; Zhao, Y.; Li, Q.; Zhang, Z.; Yang, W.; Li, Y. A review on process parameter influence and optimization for 3D printing of fiber-reinforced thermoplastic composites. *J. Reinf. Plast. Compos.* **2024**. [CrossRef]
6. Luan, C.; Yao, X.; Liu, C.; Lan, L.; Fu, J. Self-monitoring continuous carbon fiber reinforced thermoplastic based on dual-material three-dimensional printing integration process. *Carbon* **2018**, *140*, 100–111. [CrossRef]
7. Han, S.; Li, S.; Song, X.; Zhou, Z.; Meng, Q.; Araby, S.; Abdelsalam, A.A. Carbon nanotubes/α-ZrP sheets for high mechanical performance and flame-retarding polyamides using selective laser sintering. *Virtual Phys. Prototyp.* **2024**, *19*, e2368644. [CrossRef]
8. Han, S.; Li, S.; Liu, D.; Dong, Y.; Gao, Z.; Zhang, Y.; Meng, Q. Enhancing flame retardancy, anti-impact, and corrosive resistance of TPU nanocomposites using surface decoration of α-ZrP. *Polym. Compos.* **2024**, *45*, 9209–9223. [CrossRef]
9. Zhang, Y.; Zheng, T.; Liu, G.; Lu, H.; Li, G.; Zong, Q.; Gao, Y.; Zhang, W. Predicting the fatigue life of T800 carbon fiber composite structural component based on fatigue experiments of unidirectional laminates. *Int. J. Fatigue* **2025**, *190*, 108622. [CrossRef]
10. Nohair, B.; Dufresne, S.; Poirier, D.; Turgeon, M.; Elbouazzaoui, S. Hot melt thermoset/thermoplastic hybrid prepregs: Effects of B-stage conditions on the quality of composite parts. *Polym. Compos.* **2024**, *46*, 208–218. [CrossRef]
11. Nam, T.H.; Goto, K.; Kamei, T.; Shimamura, Y.; Inoue, Y.; Kobayashi, S.; Ogihara, S. Improved mechanical properties of aligned multi-walled carbon nanotube/thermoplastic polyimide composites by hot stretching. *J. Compos. Mater.* **2019**, *53*, 1241–1253. [CrossRef]
12. Cho, Y.; Kang, J.; Huh, M.; Yun, S.I. Styrene-free synthesis and curing behavior of vinyl ester resin films for hot-melt prepreg process. *Mater. Today Commun.* **2022**, *30*, 103143. [CrossRef]
13. Wu, C.; Xu, F.; Wang, H.; Liu, H.; Yan, F.; Ma, C. Manufacturing Technologies of Polymer Composites—A Review. *Polymers* **2023**, *15*, 712. [CrossRef] [PubMed]
14. Han, S.; Yang, F.; Meng, Q.; Li, J.; Sui, G.; Su, X.; Kuan, H.-C.; Wang, C.H.; Ma, J. Using renewable phosphate to decorate graphene nanoplatelets for flame-retarding, mechanically resilient epoxy nanocomposites. *Progress. Org. Coat.* **2023**, *182*, 107658. [CrossRef]
15. Korobeinyk, A.V.; Whitby, R.L.D.; Salvage, J.P.; Mikhalovsky, S.V. Exfoliated production of single- and multi-layer graphenes and carbon nanofibres from the carbonisation of a co-polymer. *Carbon* **2012**, *50*, 2018–2025. [CrossRef]
16. Peng, G.; Shi, F.; Wang, Y.; Li, G.; Zheng, H.; Zhang, B.; Xie, F.-Y. Effects of three types of T700 carbon fiber on the mechanical properties of their composites with bismaleimide resin. *New Carbon. Mater.* **2016**, *31*, 176–181.
17. Gao, Q.; Jing, M.; Wang, C.; Zhao, S.; Chen, M.; Qin, J. Preparation of High-Quality Polyacrylonitrile Precursors for Carbon Fibers Through a High Drawing Ratio in the Coagulation Bath During a Dry-Jet Wet Spinning Process. *J. Macromol. Sci. Part B Phys.* **2019**, *58*, 128–140. [CrossRef]
18. Ouyang, Q.; Chen, Y.; Wang, X.; Ma, H.; Li, D.; Yang, J. Supramolecular structure of highly oriented wet-spun polyacrylonitrile fibers used in the preparation of high-performance carbon fibers. *J. Polym. Res.* **2015**, *22*, 229. [CrossRef]
19. Xiao, M.; Li, N.; Ma, Z.; Song, H.; Lu, K.; Li, A.; Meng, Y.; Wang, D.; Yan, X. The effect of doping graphene oxide on the structure and property of polyimide-based graphite fibre. *RSC Adv.* **2017**, *7*, 56602–56610. [CrossRef]
20. Shirvan, A.R.; Nouri, A.; Sutti, A. A perspective on the wet spinning process and its advancements in biomedical sciences. *Eur. Polym. J.* **2022**, *181*, 111681. [CrossRef]
21. Wang, B.; Gao, H.; Wu, H.; Wu, Y.; Ren, B.; Liu, X.; Nie, Y. Diffusion coefficients during regenerated cellulose fibers formation using ionic liquids as solvents: Experimental investigation and molecular dynamics simulation. *Chem. Eng. J.* **2024**, *488*, 151175. [CrossRef]
22. Wang, L.; Lundahl, M.J.; Greca, L.G.; Papageorgiou, A.C.; Borghei, M.; Rojas, O.J. Effects of non-solvents and electrolytes on the formation and properties of cellulose I filaments. *Sci. Rep.* **2019**, *9*, 16691. [CrossRef] [PubMed]
23. Wang, B.; Nie, Y.; Kang, Z.; Liu, X. Effects of coagulating conditions on the crystallinity, orientation and mechanical properties of regenerated cellulose fibers. *Int. J. Biol. Macromol.* **2023**, *225*, 1374–1383. [CrossRef] [PubMed]

24. Salahi, A.; Mohammadi, T.; Behbahani, R.M.; Hemmati, M. Preparation and Performance Evaluation of Polyethersulfone Hollow Fiber Membranes for Ultrafiltration Processes. *Polym-Plast. Technol. Eng.* **2015**, *54*, 1468–1482. [CrossRef]
25. Zhao, C.; Yang, B.; Han, J.; Meng, Y.; Yu, L.; Hou, D.; Wang, J.; Zhao, Y.; Zhai, Y.; Wang, S.; et al. Preparation of carboxylic multiwalled-carbon-nanotube-modified poly(m-phenylene isophthalamide) hollow fiber nanofiltration membranes with improved performance and application for dye removal. *Appl. Surf. Sci.* **2018**, *453*, 502–512. [CrossRef]
26. Wieland, M.; Arne, W.; Feßler, R.; Marheineke, N.; Wegener, R. An efficient numerical framework for fiber spinning scenarios with evaporation effects in airflows. *J. Comput. Phys.* **2019**, *384*, 326–348. [CrossRef]
27. *QJ971A-2011*; Test Methods for Tensile Properties of Small Specimens of Fiber Reinforced Plastics. National Standards of the People's Republic of China: Beijing, China, 2011; pp. 1–8.
28. *GB/T3356-1999*; Test Method for Flexural Properties of Unidirectional Fiber Reinforced Plastics. National Standards of the People's Republic of China: Beijing, China, 1999; pp. 1–6.
29. *JC/T773-2010*; Fiber-Reinforced Plastics Determination of Interlaminar Shear Strength by Short Beam Method. National Standards of the People's Republic of China: Beijing, China, 2011; pp. 1–9.